Bioactive lipids as key regulators in atherosclerosis

Bot, M.

4 Lipid Cartography of Mouse Atherosclerotic Plaques by Cluster-TOF-SIMS Imaging

Martine Bot[1], Luke McAleese[2], Ilze Bot[1], Theo J.C. van Berkel[1], Ron M.A. Heeren[2] and Erik A.L. Biessen[1,3]

[1]Division of Biopharmaceutics, Gorlaeus Laboratories, Leiden University, Leiden, The Netherlands, [2]FOM Institute for Atomic and Molecular Physics (AMOLF), Amsterdam, The Netherlands, [3]Department of Pathology, Maastricht University, Maastricht, the Netherlands.

Manuscript in preparation

Abstract

Vascular lipid accumulation is an atherogenic pathological consequence of serum dyslipidemia. Extravasation of VLDL and LDL facilitates plaque lipid accumulation, while HDL exerts a protective function. Regardless of the mode of entry, vascular lipid deposits will not only affect the biomechanical integrity, but also the ongoing inflammatory processes and thrombogenicity of the plaque. Particularly in advanced atherosclerotic lesions, specific lipids might form a high risk area for plaque instability and rupture. A detailed analysis of lipid composition and distribution pattern among plaques is essential to identify high risk areas for plaque instability.
Here, we have applied imaging mass spectrometry (IMS) via time-of-flight secondary ion mass spectrometry (TOF-SIMS) for verification and spatial localization of lipids, and in particular the highly thrombogenic lysophosphatidic acid (LPA), in carotid artery lesions from LDLr$^{-/-}$ mice. For the identification of mouse atherosclerotic oxidized (phospho)lipids, reference lipid samples were simultaneously analyzed. IMS yielded spatial and chemical information of each analyte detected. For instance, fatty acids, cholesterol, phosphocholine, LPA species, phosphatidic acids, sphingosine 1-phosphate (S1P) and triglycerides all could be detected and localized within the plaque. Atherosclerotic plaques showed strong phosphate and phosphocholine accumulation in the cell-rich regions of the lesion. The majority of plaque lipids such as cholesterol and LPA, but surprisingly also S1P, were deposited mainly in the non-nucleated regions of the lesion, representing the necrotic core. The valuable information generated in this study warrants further research using IMS, with TOF-SIMS, in unraveling the specific composition of atherosclerotic lesions, and particularly the composition of high risk areas for plaque instability and rupture.

Introduction

Atherosclerosis is a chronic, lipid-driven inflammatory disease affecting arterial blood vessels. Lipids traditionally have been viewed as constituent of the intimal thickening, but this paradigm has shifted and nowadays lipids are not only integral building blocks of the lesion, but also appear to be active players in many processes crucial to the pathogenesis of the disease[1]. In all stages of atherosclerosis, lipids accumulate in the intimal layer to promote apoptosis and reactive oxygen species (ROS) production and ensuing lipid oxidation, smooth muscle cell proliferation and the up-regulation of pro-inflammatory genes[2]. Various lipid classes have been implicated in the processes that lead to atherosclerotic lesion progression. Oxysterols, e.g. 7-ketocholesterol, are derivatives of cholesterol and have been suggested to play an active role in atherosclerosis development in part by ROS-induced apoptosis of cells[3-5]. Oxidized phospholipids have been implicated in atherosclerosis by the association of high plasma levels of these oxidized phospholipids with increased risk of cardiovascular events[6]. In addition, particular species of oxidized phospholipids, such as those derived from 1-palmitoyl-2-arachidonoyl-sn-glycero-3-phosphocholine (oxPAPC), have been demonstrated to induce the production of chemotactic factors, such as interleukin-8, by endothelial cells[7].

In advanced atherosclerotic lesions and in particular in unstable plaques, consisting of a large lipid core and an overlying thin fibrous cap, lipids are deposited extracellularly rather than intracellularly and represent a rich source of thrombogenic activity. These unstable plaques are considered vulnerable to rupture[8,9]. Upon rupture of the fibrous cap, the thrombogenic lipid content of the plaque will be exposed to the blood circulation and trigger the coagulation cascade, leading to thrombus formation and acute coronary syndromes[10,11]. Phosphatidylserine (PS) is a phospholipid that has been implicated in this process by augmentation of the procoagulant activity of tissue factor (TF), the main cellular initiator of blood coagulation[12]. Membrane microparticles (MP) shed by apoptotic cells are sequestered within the atherosclerotic plaque and contain PS and TF, which upon plaque rupture will be exposed to the blood circulation and lead to thrombus formation[12]. Also a major thrombogenic constituents of the lipid core was demonstrated to be lysophosphatidic acid (LPA)[13-15], a group of bioactive lysolipid species consisting of a glycerol backbone, with either a saturated or an unsaturated fatty acid bonded to the carbon-1 or -2 position and a phosphate group bonded to carbon-3. LPA was shown to be an important mediator of prothrombotic actions attributed to low-density lipoprotein (LDL)[13]. In contrast, high-density lipoprotein (HDL) contains a structurally related sphingolipid, sphingosine 1-phosphate (S1P), which is at least in part responsible for the anti-atherogenic effects of HDL[16].

Thus, the specific spatial localization and identification of lipids and oxidized lipids but also that of specific cell components, enzymes and cytokines in atherosclerotic lesions is of great importance for identification of high risk areas within an atherosclerotic vessel. Molecular imaging techniques are emerging that provide more detailed information on the spatial and dynamical configuration of the diseased vessel wall and that give gross insights into the composition and biomechanical features of an atherosclerotic plaque. With appropriate targeted contrast agents or probes even localization of marker proteins or processes in lesion-prone areas, intraplaque ves-

sels and plaque-associated thrombi comes within reach, but precise knowledge of the chemical composition of the vessel wall is often limited[17]. Antibodies and fluorescent probes[18,19] have frequently been used for assessing the localization of lipids in atherosclerotic lesions but sample preparation[20] and probe specificity are commonly encountered sources of artefacts[21]. Imaging mass spectrometry has emerged as a promising technique for the compositional analysis of tissue sections, as it allows chemical identification and localization of unknown surface molecules with excellent spatial resolution[22-26]. In recent years, optimization of sample preparation techniques has led to enhanced detection of intact molecules[27], clearly increasing the potential of biomolecular surface imaging by time-of-flight secondary ion mass spectrometry (TOF-SIMS). Here, we set out to apply imaging mass spectrometry to visualize intraplaque lipid distribution patterns and to identify high risk areas within the carotid artery lesion from LDL receptor deficient ($LDLr^{-/-}$) mice, a mouse model for atherosclerotic lesion formation with a human-like lipoprotein pattern.

Methods

Animals

All animal work was approved by the regulatory authority of Leiden University and performed in compliance with Dutch government guidelines. Male $LDLr^{-/-}$ mice, obtained from Jackson Laboratories and bred in our local animal breeding facility, were fed a Western type diet containing 0.25% cholesterol and 15% cocoa butter (Special Diet Services, Sussex, UK) two weeks prior to surgery and throughout the experiment. The spatial lipid composition of mouse plaques was visualized in atherosclerotic carotid artery lesions induced by perivascular collar placement as described previously[28]. Mice were anesthetized by subcutaneous injection of ketamine (60 mg/kg, Eurovet Animal Health, Bladel, The Netherlands), fentanyl citrate and fluanisone (1.26 mg/kg and 2 mg/kg respectively, Janssen Animal Health, Sauderton, UK).

Tissue harvesting

Lipid distribution of carotid artery plaques in $LDLr^{-/-}$ mice was determined at 9 weeks after perivascular collar placement. Hereto, mice were sacrificed by perfusion through the left cardiac ventricle with phosphate buffered saline (150 mM NaCl, 1.5 mM NaH_2PO_4, 8.6 mM Na_2HPO_4, pH 7.4) followed by perfusion with 0.128 M ammonium bicarbonate to remove salts which interfere with SIMS measurements. Subsequently, the common carotid arteries were both excised, embedded in 10% gelatin at 30ºC and snap-frozen in liquid nitrogen for optimal lipid preservation. The specimens were stored at -80°C until further use. Transverse 10 µm cryosections were prepared on a Leica CM 3050 cryostat (Leica microsytems, Rijswijk, the Netherlands) at -20 ºC. The sections were cut in a proximal direction from the carotid bifurcation and mounted in order on a parallel series of glass slides, alternating between 1% gelatin coated slides for immunohistological staining and conductive, transparent indium tin oxide (ITO)-coated slides (Delta Technologies, Stillwater, MN, USA) for TOF-SIMS, which are stored at -80°C until further use. Conservation of morphology was checked by optical microscopy during the sectioning process.

Histology
A series of sections on a gelatin-coated slide were stained with hematoxylin (Sigma Diagnostics, Zwijndrecht, the Netherlands) and eosin (Merck Diagnostica, Darmstadt, Germany). A consecutive series of sections on a gelatin-coated slide were stained immunohistochemically with antibodies directed against mouse macrophages (monoclonal mouse IgG_{2a}, clone monocyte + macrophage antibody-2 [MOMA-2], dilution 1:50; Sigma Diagnostics).

Gold Deposition
The sample surface of a series of sections mounted on conductive slides were sputter coated with gold using a Quorum Technologies (Newhaven, East Sussex, UK) SC7640 sputter coater.

Reference samples
18:1/18:1 PA (Sigma-Aldrich, Zwijndrecht, the Netherlands), 18:1 LPA (Sigma-Aldrich) and S1P (Cayman chemical, MI, USA) were dissolved in methanol 100% and 80%, respectively, and prepared by droplet deposition onto a clean steel metal holder before mass spectrometry analysis. Mass spectrometry analysis was performed with SIMS and matrix-enhanced SIMS (ME-SIMS). For ME-SIMS matrix was deposited by electrospray preparation with either 2,5-dihydroxybenzoic acid (DHB) or α-cyano-4-hydroxycinamic acid (HCCA).

Mass spectrometry
All static SIMS experiments were performed on a Physical Electronics (Eden Prairie, MN, USA) TRIFT-II time-of-flight SIMS (TOF-SIMS) instrument described elsewhere[27] and newly equipped with a gold liquid metal ion gun. Secondary ions were extracted through a 3.2 keV electric field into the TOF analyzer and post-accelerated by an additional 8 keV field prior to detection on a dual multichannel plate/phosphor screen detector. All experiments were performed with a primary ion beam current of 1 nA, a primary pulse length of 18 ns and a primary ion energy of 22 keV. The ion dose was such that all analyses were conducted at or under the static SIMS threshold (10^{13} ions/cm^2) for reduced fragmentation of analytes. The instrument was calibrated in both positive and negative mode on high occurrence elements and fragments such as $H^{+/-}$, CH^{n+}, Na^+, K^+, O^-, OH^-.
An image is measured by rastering, in a 256*256 position pattern, a focused primary ion beam on the sample surface, in a tile of adjustable dimension (below 150 microns) and recording the mass spectra together with the position of the primary ion beam in the raster. In the so called mosaic mode, large areas are measured by dividing them in a mosaic of such tiles measured successively, moving the sample between each tile. For all lipid standards, both in positive and negative mode, measurements of 15 seconds per tile of a small mosaic of 4*4 tiles of 125 microns were acquired in order to average the mass spectrum on a large surface. This will reduce unevenness of distribution due to sample preparation. For measurement of artery sections, mosaics of 8*8 tiles of 67.5 microns each were measured, forming total images of 540*540 micron, large enough to fully enclose each artery section. Images were acquired both in positive and negative mode and without or with gold coating (1 nm, meta-SIMS). Spatial resolution of the mass spectrometry images was around 1

micron. The chemical images were compared to histological images of consecutive sections.

Ion identification

Lipidomic analyses of plaque lipid pools and reference lipids performed at the department of biochemistry and cell biology of the Utrecht university enabled us to identify individual LPA species, which appeared by electrospray ionization (ESI) as $[M-H]^-$ anions as described in chapter 3 of this thesis (Table 1).

LPA	molecular weight	detected anion as in chapter 3 $[M-H]^-$
14:0	382.3	381.3
16:1	408.3	407.3
16:0	410.3	409.3
18:3	432.3	431.3
18:2	434.3	433.3
18:1	436.3	435.3
18:0	438.3	437.3
20:3	458.4	457.4
20:2	460.4	459.4
22:5	480.4	479.4
22:4	482.4	481.4

Table 1. Negative mode *m/z* from LPA species identified by ESI at the department of biochemistry and cell biology of the Utrecht university.

Assignment negative mode		expected ion	expected ion mass
CN^-		-	26
CNO^-		-	43
PO_2^-		-	63
PO_3^-		-	79
SO_2^-		-	64
SO_3^-		-	80
NEFA	Palmitic (16:0)	$[M-H]^-$	255.2
	Palmitoleic (16:1)	$[M-H]^-$	253.2
	Hexadecadienoic (16:2)	$[M-H]^-$	251.2
	Stearic (18:0)	$[M-H]^-$	283.2
	Oleic (18:1)	$[M-H]^-$	281.2
	Linoleic (18:2)	$[M-H]^-$	279.2
	Gamma-linolenic (18:3)	$[M-H]^-$	277.2
	Arachidonic (20:4)	$[M-H]^-$	303.2
Cholesterol		$[M-H]^-$	385.4
LPA(17:1)		$[M-H]^-$	421.3
Sphingosine		$[M-H]^-$	298.3
Sphingosine 1-phosphate		$[M-H]^-$	378.3
Sphinganine		$[M-H]^-$	300.3
Sphinganine-phosphate		$[M-H]^-$	380.3
Phosphatidic Acids		-	650-750
Triglycerides		-	829-882
Vitamin E		-	429.4

Assignment positive mode	expected ion	expected ion mass
Na^+	-	23
K^+	-	39
Glycerophosphatidylcholine fragment	-	86
Phosphocholine headgroup	-	184
Cholesterol	$[M+H-H_2O]^+$	369.3
Cholesterol	$[M-H]^+$	385.4

Table 2. Expected/theoretical masses (*m/z*) of anorganic and lipid plaque constituents as assessed by negative and positive mode image mass spectrometry. NEFA; non-esterified fatty acids.

Lipid species expected to be present in and of importance to atherosclerosis were searched for on the basis of their potential ion mass with similar ionization pathways as observed in literature[25,26,29-32] and from previous experiments, including several ionizing sources (ESI at Utrecht, electron impact (EI) in the LIPID Metabolites And Pathways Strategy spectra database, and SIMS/ME-SIMS performed in the lab on standards) (Table 1 and 2). Mass selected images were extracted from the full IMS dataset and specific localization lead to discussion and interpretation from a biological point of view. However, it must be noted that as no MS/MS has been performed the actual molecular assignment of mass peaks should be taken with caution at this stage.

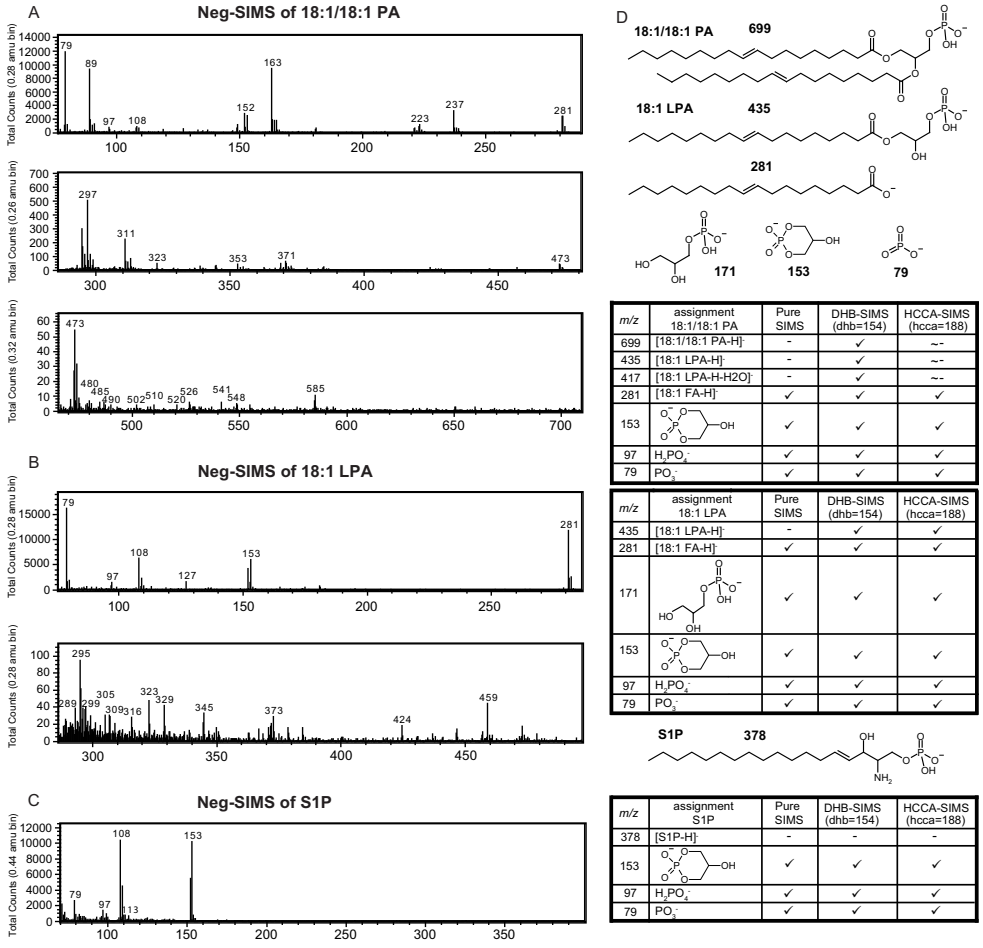

m/z	assignment 18:1/18:1 PA	Pure SIMS	DHB-SIMS (dhb=154)	HCCA-SIMS (hcca=188)
699	[18:1/18:1 PA-H]$^-$	-	✓	~-
435	[18:1 LPA-H]$^-$	-	✓	~-
417	[18:1 LPA-H-H2O]$^-$	-	✓	~-
281	[18:1 FA-H]$^-$	✓	✓	✓
153		✓	✓	✓
97	$H_2PO_4^-$	✓	✓	✓
79	PO_3^-	✓	✓	✓

m/z	assignment 18:1 LPA	Pure SIMS	DHB-SIMS (dhb=154)	HCCA-SIMS (hcca=188)
435	[18:1 LPA-H]$^-$	-	✓	✓
281	[18:1 FA-H]$^-$	✓	✓	✓
171		✓	✓	✓
153		✓	✓	✓
97	$H_2PO_4^-$	✓	✓	✓
79	PO_3^-	✓	✓	✓

m/z	assignment S1P	Pure SIMS	DHB-SIMS (dhb=154)	HCCA-SIMS (hcca=188)
378	[S1P-H]$^-$	-	-	-
153		✓	✓	✓
97	$H_2PO_4^-$	✓	✓	✓
79	PO_3^-	✓	✓	✓

Figure 1. Reference sample analysis in negative mode SIMS. (A) SIMS spectrum of 18:1/18:1 PA. (B) SIMS spectrum of 18:1 LPA. (C) SIMS spectrum of S1P. (D) Chemical structures of the reference compounds and their theoretical fragmentation patterns. The tables show *m/z* of the detected fragmentation products of PA, LPA and S1P and detection in SIMS and ME-SIMS (using matrices DHB or HCCA).

Results

Reference lipids in SIMS

SIMS analysis shows strong signals for inorganic ions and ionized organic compounds derived from fragmentation of surface molecules. As shown before[27], the use of gold coating (meta-SIMS) resulted in great enhancement of the sensitivity for assessment of middle to high mass range compounds (>200 *m/z*) in tissue. To ensure correct identification of the lipid species of interest, reference samples of 18:1/18:1 PA, 18:1 LPA and S1P were analyzed with SIMS and ME-SIMS. Negative polarity reference spectra from the reference samples are shown in figure 1A-C. Figure 1D shows the chemical structures of the reference compounds, their theoretical fragmentation pattern and the corresponding *m/z* in the negative ion mode.

Imaging mass spectrometry of carotid artery plaques by SIMS

Surface rastering of atherosclerotic carotid artery sections generated multiple secondary ions in the *m/z* range between 1 and 1000, corresponding mostly to singly charged ions. The lower mass peaks (<200 *m/z*) in positive mode showed the presence of phosphocholine-containing phospholipids such as phosphatidylcholine which could be identified by characteristic fragmentation products such as a glycerophosphatidylcholine fragment at *m/z* 86 and phosphocholine headgroup (*m/z* 184). Cholesterol could be detected in the intermediate mass peaks (*m/z* 200 to 500) through the well-defined peak at *m/z* 369 $[M+H-H2O]^+$ and a minor peak at *m/z* 385 $[M-H]^+$ (Figure 2). In the negative mode, SIMS spectra in the lower mass region were dominated by CN^-, CNO^- and various phosphates, such as PO_2^- (*m/z* 63) and PO_3^- (*m/z* 79), and sulfur-containing ions, such as SO_2^- and SO_3^-.

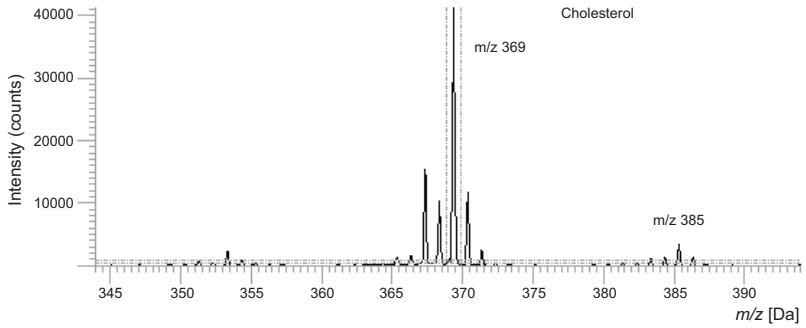

Figure 2. TOF-SIMS spectrum of cholesterol recorded from an atherosclerotic artery segment in positive mode.

Fatty acids could be typically detected as $[M-H]^-$ in the negative mode (Figure 3A). The *m/z* mid-range showed several peaks that were tentatively assigned to non-esterified fatty acids: palmitic (C16:0, *m/z* 255), palmitoleic (C16:1, *m/z* 253), stearic (C18:0, *m/z* 283), oleic (C18:1, *m/z* 281), linoleic (18:2, *m/z* 279), gamma-linolenic (C18:3, *m/z* 277) or arachidonic (C20:4, *m/z* 303). Also cholesterol gave a well-defined peak at *m/z* 385 in negative mode. As we were particularly interested in the

spatial distribution and accumulation of LPA species, S1P and sphinganine 1-phosphate in atherosclerotic lesions, we next focused on these lipid species. Assessment of the intraplaque distribution of these lipids was performed on the basis of their intact mass anions $[M-H]^-$, as determined by LC-MS of crude plaque lipid pools like described in chapter 3 (Table 1) or obtained from literature (Table 2): 14:0 LPA (*m/z* 381) 16:0 LPA (*m/z* 409), 16:1 LPA (*m/z* 407), 17:1 LPA (*m/z* 421), 18:0 LPA (*m/z* 437), 18:1 LPA (*m/z* 435), 18:2 LPA (*m/z* 433), 18:3 LPA (*m/z* 431), 20:2 LPA (*m/z* 459), 20:3 LPA (*m/z* 457), 22:4 LPA (*m/z* 481), 22:5 LPA (*m/z* 479), sphingosine (*m/z* 298), S1P (*m/z* 378), sphinganine (*m/z* 300) and sphinganine 1-phosphate (*m/z* 380) (Figure 3B). Finally, vitamin E was imaged via its intact mass as well as the mass of one of its fragment at respectively *m/z* 429 and 157, whereas phosphatidic acids and triglycerides were detected at mass ranges *m/z* 650-750 and 829-882, respectively (Figure 3C).

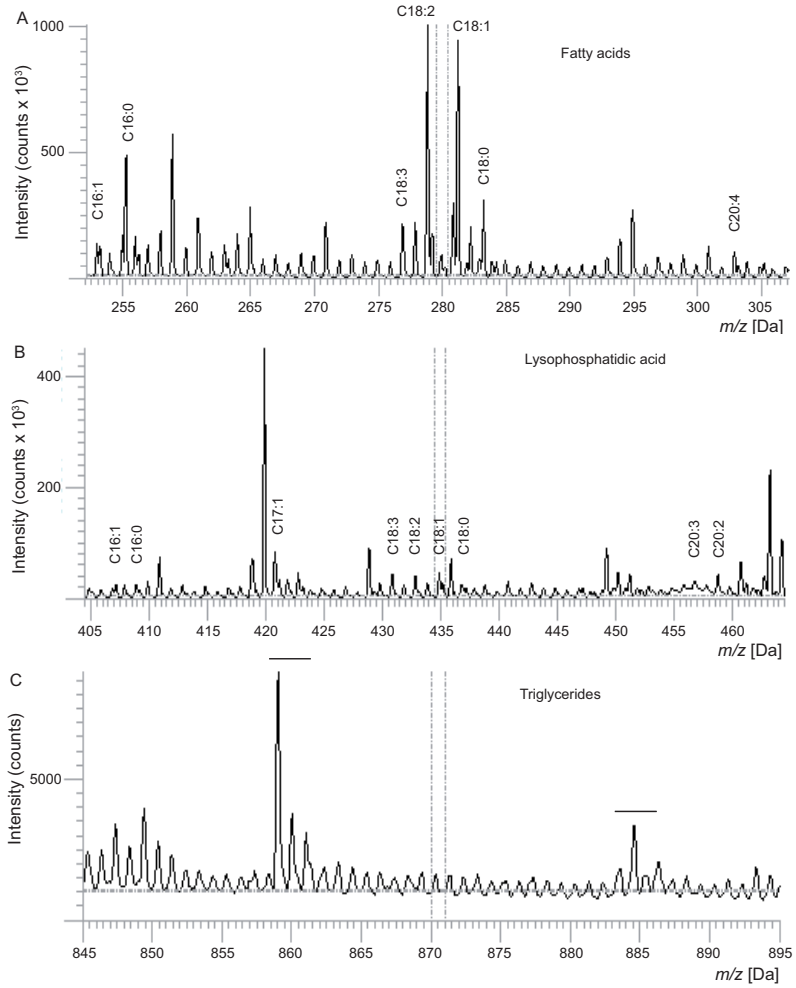

Figure 3. TOF-SIMS spectra recorded from an atherosclerotic artery segment in negative mode with tentative peak assignments: (A) Fatty acids. (B) Lysophosphatidic acid species. (C) Triglycerides.

To correlate intraplaque lipid distribution profiles to morphological features, flanking sections were stained for HE and macrophage content (Figure 4 and 5). Figure 4 displays an HE (Figure 4A) and MOMA-2 macrophage staining (Figure 4B) as well as the positive ion images (Figure 4C, 4D) of the corresponding sections for a selected set of lipids as assigned from the above defined *m/z* peaks. Color intensity of the ion micrographs corresponded to signal strength. As expected the distribution of both Na^+ and cholesterol was seen to correlate with the non-nucleated regions of the carotid artery lesion, while phosphocholine fragments derived from phosphocholine-containing phospholipids correlated with the more cellular regions of the intima.

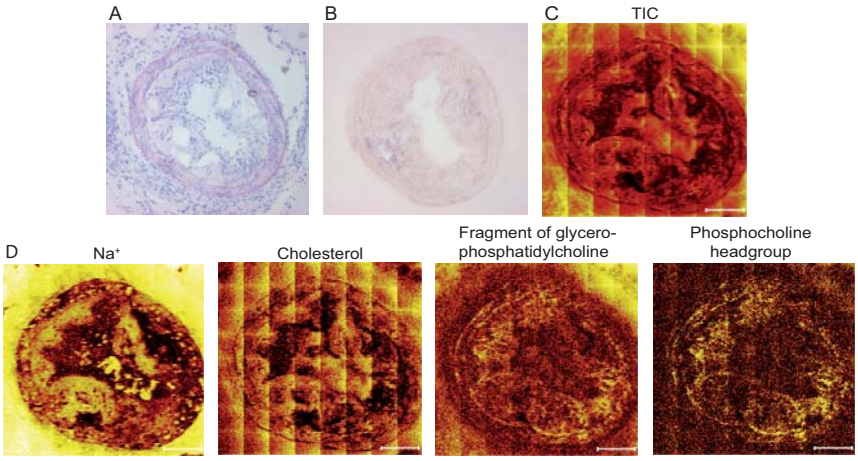

Figure 4. (A) HE staining of a mouse atherosclerotic lesion. (B) MOMA-2 staining showing presence of macrophages in the plaque section. (C,D) Positive ion micrographs of a flanking section of the atherosclerotic artery lesion analyzed by TOF-SIMS showing in artificial color the signal distribution from single ion peaks. Yellow color intensity corresponds to signal strength. (C) Total ion current (TIC). (D) Intraplaque localization of sodium, cholesterol, fragmented glycerophosphatidylcholine and phosphocholine headgroup. Scale bar indicates 100 microns.

Figure 5 displays the HE (Figure 5A) and MOMA-2 macrophage staining (Figure 5B) as well as the corresponding negative ion images (Figure 5C, 5D) of the lesion. The nucleated regions of the intima were particularly enriched in phosphates, while sulfates, non-esterified fatty acids, cholesterol, the multiple LPA species, S1P, sphinganine 1-phosphate, phosphatidic acids, triglycerides and vitamin E all showed accumulation in the non-cellular core region of the plaque, despite remarkable differences in site of synthesis and lipophilicity.

Overlay images obtained for various relevant ions by positive and negative mode spectrometry are depicted in figure 6. Overlay of positive ion micrographs clearly illustrated the divergent distribution patterns of cholesterol and choline-containing groups (Figure 6A, 6B). Likewise, the overlay of negative ion micrographs established non-overlapping distribution of cholesterol and phosphates, and colocalization of cholesterol with sulfur-containing ions (Figure 6C, 6D).

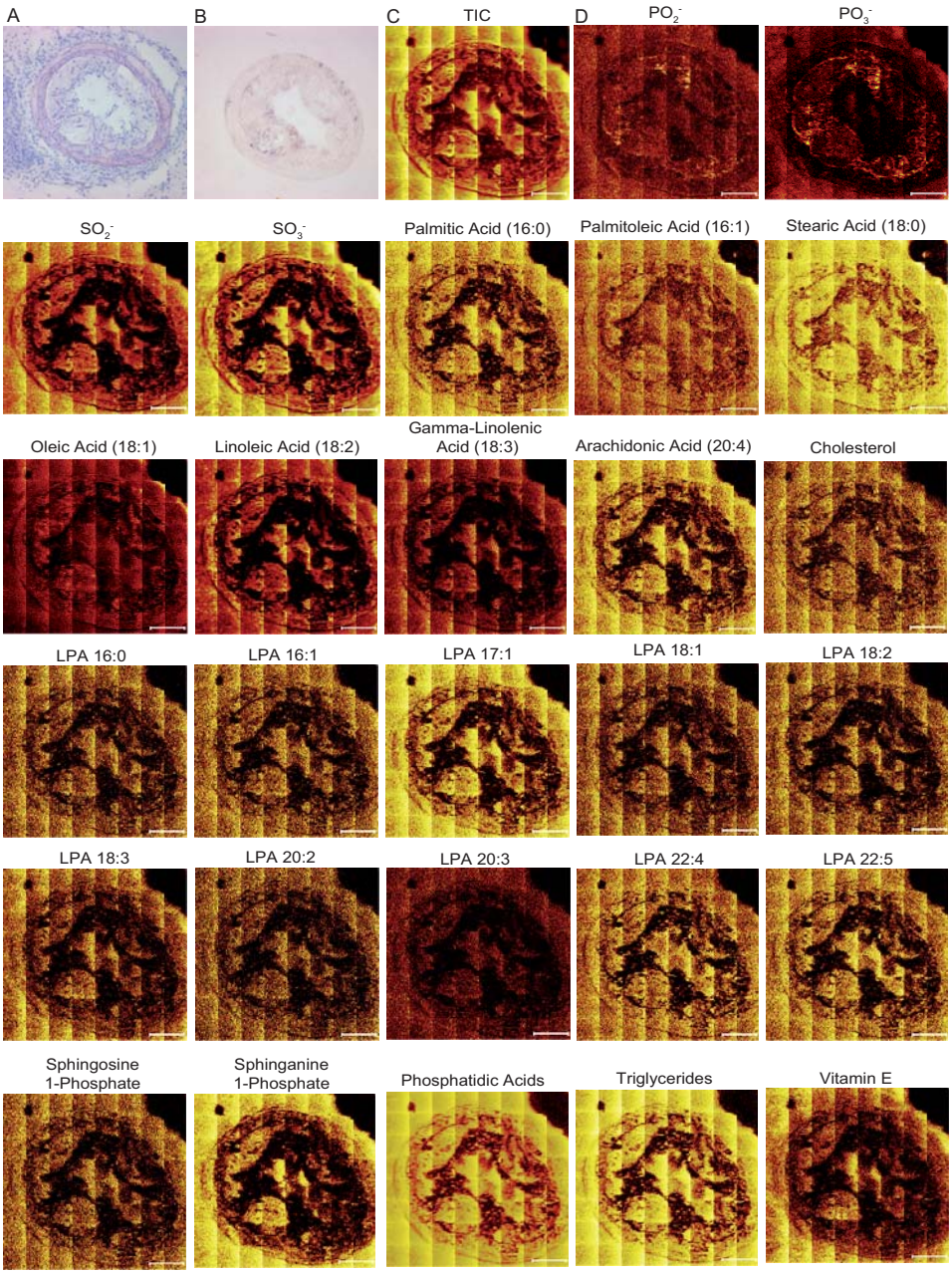

Figure 5. HE staining (A) and MOMA-2 macrophage staining (B) of a mouse carotid artery lesion. Negative ion micrographs of a flanking lesion analyzed by TOF-SIMS. Yellow color intensity corresponds to signal strength. (C) Total ion current (TIC). (D) Intraplaque distribution patterns of a selection of relevant ions including phosphates, sulfates and several lipid species. Scale bar indicates 100 microns.

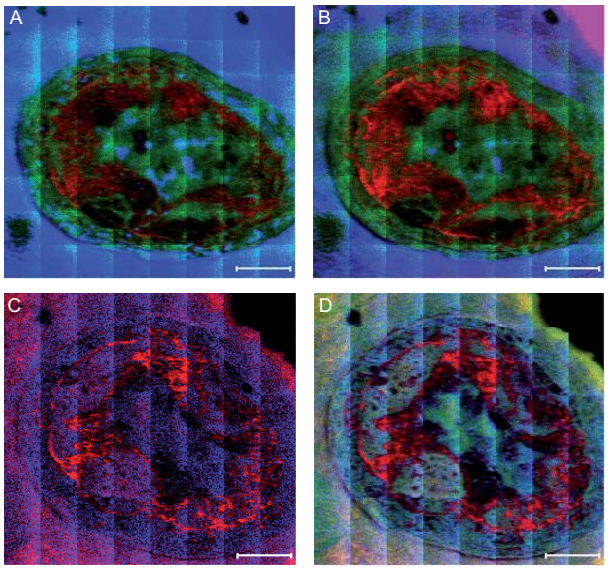

Figure 6. (A) Overlay image of phosphocholine (red), sodium (blue) and cholesterol (green) micrographs of a mouse carotid artery lesion analyzed in positive mode. (B) Overlay image of choline (red), sodium (blue) and cholesterol (green) micrographs of a mouse carotid artery lesion analyzed in positive mode. (C,D) Overlay images of phosphate (red), cholesterol (blue) and sulfate (green) micrographs of a mouse carotid artery lesion analyzed in negative mode. Scale bar indicates 100 microns.

Discussion

TOF-SIMS spatial mass spectrometry/cartography imaging allowed us to not only detect but also localize key lipids in atherogenesis such as fatty acids, cholesterol, LPA, S1P, sphinganine 1-phosphate, phosphatidic acids and triglycerides in mouse carotid artery lesions. As expected most lipids, among which highly thrombogenic LPA species, were deposited in the non-nucleated compartments of the intima, while phosphates and phosphocholine-containing phospholipids were preferentially localized in cellular regions of the atherosclerotic lesion. Previous studies have described that presence of PO_3 and phosphocholine indicate cellular contributions such as vascular smooth muscle cells[25]. The striking colocalization of phosphate and phosphocholine signals in the cellular domains of the mouse carotid artery lesion therefore suggests the presence of VSMCs, but could also indicate the influx of leukocytes such as macrophages. The spatial information on the distribution pattern of individual plaque constituents presented in this study warrants further research on image mass spectrometry, with TOF-SIMS to unravel the chemical composition of atherosclerotic lesions, and particularly of high risk plaques, potentially yielding new chemical entities for molecular imaging of the latter plaque. Moreover, it will help to detect *in situ* activity of critical enzymes or processes such as hypoxia, oxidative stress, redox potential and metabolic activity in the diseased arterial wall during atherogenesis.
The overt presence of free fatty acids and cholesterol in non-nucleated region of the intima may be lipoprotein-derived and either directly or after uptake by macrophages

deposited in the core, further illustrating the relevance of accumulation of lipoprotein particles in necrotic core formation. It also indicates that lipoprotein derived triglycerides have probably been hydrolyzed to yield free fatty acids and free cholesterol by lipases (e.g. endothelial hormone sensitive and lipoprotein lipase), and esterases, respectively, present not only at the luminal endothelium but also close to the lipid core[33]. Free fatty acids have a broad range of effects on VSMCs, and specifically palmitate and arachidonic acid, as shown in this study to be abundantly present in the intima of atherosclerotic lesions, are known to promote reactive oxygen species production by VSMCs[34] and induce apoptosis of VSMCs[35,36]. Since smooth muscle cells form the protective fibrous cap overlying the lipid-laden and thrombogenic necrotic core of atherosclerotic lesions, free fatty acid-induced apoptosis can cause cap thinning thereby contributing to plaque destabilization. Conversely, fatty acids can beneficially modulate inflammatory processes involved in atherosclerosis by activation of nuclear receptors in macrophages and VSMCs[37-39].

LPA has been shown to be an integral component of LDL and an important mediator for the pro-thrombotic actions of LDL[13], suggesting the preferential presence of this lipid at sites of LDL accumulation. Indeed, the necrotic core, the most prominent site of LDL and cholesterol accumulation, was seen to contain the majority of LPA species (as judged from the intensity of mass peaks in the SIMS spectrum that was tentatively assigned to LPA class lipids). However, LPA may not only originate from LDL accumulation but can also be formed *in situ* by lesion macrophages which display an altered LPA homeostasis favoring net synthesis (Bot *et al.*, chapter 3 of this thesis). Unfortunately, we were unable to establish colocalization of LPA deposits and MOMA-2-positive macrophages. Possibly other macrophage markers, whether by SIMS or by immunohistochemistry, may be used to pinpoint the relative portion of LPA that colocalizes with macrophages. Interestingly, also a compound which on the basis of its mass could be attributed to S1P, which in the blood is mostly associated with HDL, localized in the same core regions. Surprisingly, 7-ketocholesterol, one of the oxysterols described to be implicated in atherosclerosis development, could not be detected in the mouse carotid artery lesions. Finally, vitamin E, which has anti-oxidant properties[40], was also found to localize to lipid-rich areas in the atherosclerotic lesion. As to what extent vitamin E can be beneficial in this context, still has to be established.

Despite these promising results of IMS the data analyses should be approached with caution. Analysis of the references shows that the fragmentation patterns of LPA and PA overlap considerably rendering it difficult to assign the mass peak to one of these lipids on the basis of single MS measurements. However, references were measured in pure SIMS, while artery sections were gold-coated. Coating sections with matrix or gold enhances detection of intact molecules, as was shown previously[27], suggesting that peak masses more often refer to intact lipids than to lipid fragments in gold-coated sample mass spectra. Indeed, analysis of reference lipids with ME-SIMS improved the intact molecule signals. Nevertheless, future analyses of artery sections by ME-SIMS and subsequent matrix-assisted laser desorption/ionization (MALDI) MS/MS will help to unambiguously identify the chemical identity of the detected mass peaks in the cartography.

In conclusion, this proof-of-concept study shows that imaging mass spectrometry is a powerful technique for metabolic and compositional analysis of mouse atheroscle-

rotic plaques at high resolution. It underlines the significance of TOF-SIMS as valuable technology to unveil spatial information of a multitude of low molecular weight molecules and ions directly in biological specimen in only a single experiment, as also demonstrated for other tissues[22-26]. We, in addition, are the first to address the biologically relevant question of localization of thrombogenic lipids such as LPA within an atherosclerotic plaque. LPA-associated peaks proved to be mainly localized in the lipid-rich, non-nucleated core regions. To our surprise its related anti-atherogenic counterpart, S1P, seems to colocalize with LPA and mainly accumulates in core regions as well, despite its much lower lipophilicity, reflecting a balance of pro-atherogenic, plaque destabilizing LPA and anti-atherogenic S1P within the mouse plaque. Whether the same equilibrium holds for human lesions and at other (more advanced) stages of lesion formation in mice remains to be investigated. Nevertheless, these promising results warrant further IMS studies on atherosclerotic tissue, with TOF-SIMS as well as MALDI, to unravel the chemical composition of atherosclerotic and in particular high risk lesions and to spatially pinpoint biochemical processes within the plaque at different stages of disease development.

References

1. Berliner JA, Navab M, Fogelman AM, Frank JS, Demer LL, Edwards PA, Watson AD, Lusis AJ. Atherosclerosis: basic mechanisms. Oxidation, inflammation, and genetics. *Circulation.* 1995;91:2488-96.
2. Lusis AJ. Atherosclerosis. *Nature.* 2000;407:233-241.
3. Brown AJ, Jessup W. Oxysterols and atherosclerosis. *Atherosclerosis.* 1999 ;142:1-28.
4. Martinet W, De Bie M, Schrijvers DM, De Meyer GR, Herman AG, Kockx MM. 7-ketocholesterol induces protein ubiquitination, myelin figure formation, and light chain 3 processing in vascular smooth muscle cells. *Arterioscler Thromb Vasc Biol.* 2004;24:2296-2301.
5. Leonarduzzi G, Vizio B, Sottero B, Verde V, Gamba P, Mascia C, Chiarpotto E, Poli G, Biasi F. Early involvement of ROS overproduction in apoptosis induced by 7-ketocholesterol. *Antioxid Redox Signal.* 2006;8:375-380.
6. Kiechl S, Willeit J, Mayr M, Viehweider B, Oberhollenzer M, Kronenberg F, Wiedermann CJ, Oberthaler S, Xu Q, Witztum JL, Tsimikas S. Oxidized phospholipids, lipoprotein(a), lipoprotein-associated phospholipase A2 activity, and 10-year cardiovascular outcomes: prospective results from the Bruneck study. *Arterioscler Thromb Vasc Biol.* 2007;27:1788-1795.
7. Gharavi NM, Alva JA, Mouillesseaux KP, Lai C, Yeh M, Yeung W, Johnson J, Szeto WL, Hong L, Fishbein M, Wei L, Pfeffer LM, Berliner JA. Role of the Jak/STAT pathway in the regulation of interleukin-8 transcription by oxidized phospholipids in vitro and in atherosclerosis in vivo. *J Biol Chem.* 2007;282:31460-31468.
8. Ross R. Atherosclerosis, an inflammatory disease. *New Engl J Med.* 1999;340:115-126.
9. Libby P. Current concepts of the pathogenesis of the acute coronary syndromes. *Circulation.* 2001;104:365-372.
10. Shah PK. Mechanisms of plaque vulnerability and rupture. *J Am Coll Cardiol.* 2003;41:15S-22S.
11. Falk E. Why do plaques rupture? *Circulation.* 1992;86,III30-III42.
12. Morel O, Toti F, Hugel B, Bakouboula B, Camoin-Jau L, Dignat-George F, Freyssinet JM. Procoagulant microparticles: disrupting the vascular homeostasis equation? *Arterioscler Thromb Vasc Biol.* 2006;26:2594-2604.
13. Siess W, Zangl KJ, Essler M, Bauer M, Brandl R, Corrinth C, Bittman R, Tigyi G, Aepfelbacher M. Lysophosphatidic acid mediates the rapid activation of platelets and endothelial cells by mildly oxidized low density lipoprotein and accumulates in human atherosclerotic lesions. *Proc Natl Acad Sci U S A.* 1999;96:6931-6936.
14. Rother E, Brandl R, Baker DL, Goyal P, Gebhard H, Tigyi G, Siess W. Subtype-selective antagonists of lysophosphatidic acid receptors inhibit platelet activation triggered by the lipid core of atherosclerotic plaques. *Circulation.* 2003;108:741-747.
15. Siess W, Tigyi G. Thrombogenic and atherogenic activities of lysophosphatidic acid. *J Cell Biochem.* 2004;92:1086-1094.
16. Nofer JR, Assmann G. Atheroprotective effects of high-density lipoprotein-associated lysosphingolipids. *Trends Cardiovasc Med.* 2005;15:265-271.
17. Sanz J, Fayad ZA. Imaging of atherosclerotic cardiovascular disease. *Nature.* 2008;451:953-7.
18. Bugelski PJ, Maleeff BE, Klinkner AM, Louden CS, Hart TK. Nonlinear Dynamics in the Progression of Atherosclerotic Fatty Streaks: Morphometric Analysis. *Microsc Microanal.* 2000;6:532–541.
19. Bobryshev YV, Lord RS. Accumulation of co-localised unesterified cholesterol and neutral lipids within vacuolised elastin fibres in atheroprone areas of the human aorta. *Atherosclerosis.* 1999;142:121–131.
20. Maneta-Peyret L, Compere P, Moreau P, Goffinet G, Cassagne C. Immunocytochemistry of lipids: chemical fixatives have dramatic effects on the preservation of tissue lipids. *Histochem J.* 1999;31:541–547.
21. Mukherjee S, Zha X, Tabas I, Maxfield FR. Cholesterol distribution in living cells: fluorescence imaging using dehydroergosterol as a fluorescent cholesterol analog. *Biophys J.* 1998;75:1915–1925.
22. McDonnell LA, Piersma SR, MaartenAltelaar AF, Mize TH, Luxembourg SL, Verhaert PD, van Minnen J, Heeren RM. Subcellular imaging mass spectrometry of brain tissue. *J Mass Spectrom.* 2005;40:160-168.
23. McDonnell LA, Heeren RM. Imaging mass spectrometry. *Mass Spectrom Rev.* 2007;26:606-643.
24. Nygren H, Börner K, Malmberg P, Hagenhoff B. Localization of cholesterol in rat cerebellum with imaging TOF-SIMS: Effect of tissue preparation. *Applied Surface Science.* 2006;252:6975-6981.
25. Malmberg P, Börner K, Chen Y, Friberg P, Hagenhoff B, Månsson JE, Nygren H. Localization of lipids in the aortic wall with imaging TOF-SIMS. *Biochim Biophys Acta.* 2007;1771:185-195.
26. Mas S, Touboul D, Brunelle A, Aragoncillo P, Egido J, Laprévote O, Vivanco F. Lipid cartography of atherosclerotic plaque by cluster-TOF-SIMS imaging. *Analyst.* 2007;132:24-26.
27. Altelaar AF, Klinkert I, Jalink K, de Lange RP, Adan RA, Heeren RM, Piersma SR. Gold-enhanced

biomolecular surface imaging of cells and tissue by SIMS and MALDI mass spectrometry. *Anal Chem.* 2006;78:734-742.
28. von der Thüsen JH, van Berkel TJC, Biessen EAL. Induction of rapid atherogenesis by perivascular carotid collar placement in apolipoprotein E-deficient and low-density lipoprotein receptor-deficient mice. *Circulation.* 2002;103:1164-1170.
29. Touboul D, Brunelle A, Laprévote O. Structural analysis of secondary ions by post-source decay in time-of-flight secondary ion mass spectrometry. *Rapid Commun Mass Spectrom.* 2006;20:703-709.
30. Monroe EB, Jurchen JC, Lee J, Rubakhin SS, Sweedler JV. Vitamin E imaging and localization in the neuronal membrane. *J Am Chem Soc.* 2005;127:12152-12153.
31. Roddy TP, Cannon DM Jr, Ostrowski SG, Ewing AG, Winograd N. Proton transfer in time-of-flight secondary ion mass spectrometry studies of frozen-hydrated dipalmitoylphosphatidylcholine. *Anal Chem.* 2003;75:4087-4094.
32. Jones EA, Lockyer NP, Vickerman JC. Depth profiling brain tissue sections with a 40 keV C60+ primary ion beam. *Anal Chem.* 2008;80:2125-2132.
33. Hasham SN, Pillarisetti S. Vascular lipases, inflammation and atherosclerosis. *Clin Chim Acta.* 2006;372:179-183.
34. Inoguchi T, Li P, Umeda F, Yu HY, Kakimoto M, Imamura M, Aoki T, Etoh T, Hashimoto T, Naruse M, Sano H, Utsumi H, Nawata H. High glucose level and free fatty acid stimulate reactive oxygen species production through protein kinase C--dependent activation of NAD(P)H oxidase in cultured vascular cells. *Diabetes.* 2000;49:1939-1945.
35. Kalyankrishna S, Parmentier JH, Malik KU. Arachidonic acid-derived oxidation products initiate apoptosis in vascular smooth muscle cells. *Prostaglandins Other Lipid Mediat.* 2002;70:13-29.
36. Artwohl M, Lindenmair A, Roden M, Waldhäusl WK, Freudenthaler A, Klosner G, Ilhan A, Luger A, Baumgartner-Parzer SM. Fatty acids induce apoptosis in human smooth muscle cells depending on chain length, saturation, and duration of exposure. *Atherosclerosis.* 2008 May 28. Epub ahead of print.
37. Fruchart JC, Duriez P, Staels B. Peroxisome proliferator-activated receptor-alpha activators regulate genes governing lipoprotein metabolism, vascular inflammation and atherosclerosis. *Curr Opin Lipidol.* 1999;10:245-257.
38. Chinetti G, Lestavel S, Fruchart JC, Clavey V, Staels B. Peroxisome proliferator-activated receptor alpha reduces cholesterol esterification in macrophages. *Circ Res.* 2003;92:212-217.
39. Reddy RC. Immunomodulatory role of PPAR-gamma in alveolar macrophages. *J Investig Med.* 2008;56:522-527.
40. Packer L, Weber SU, Rimbach G. Molecular aspects of alpha-tocotrienol antioxidant action and cell signalling. *J Nutr.* 2001;131:369S-373S.